Enhanced heat transfer in channels with staggered fins of different spacings

M. A. Habib
Mechanical Engineering Department, King Fahd University of Petroleum and Minerals, Dhahran, Saudi Arabia

A. M. Mobarak, A. M. Attya and A. Z. Aly
Mechanical Engineering Department, Faculty of Engineering, Cairo University, Egypt

The flow pattern and heat transfer across staggered fins inside a rectangular duct are presented. The influence of Reynolds number, fin spacing, fin material, and wall heat flux on local and average heat transfer coefficients are studied. Fin spacings ranged from 0.8 to 2.0 times the channel height. The fin height was 0.7 times the channel height. The investigated Reynolds number ranged from 8,000 to 18,000. The experimental results show that the flow must pass over three to six fins before it appears to be a thermally periodic, fully developed flow. The fins enhance the heat transfer significantly due to flow deflection and impingement upon the fins. Augmentation of heat transfer was obtained with increase in Reynolds number, thermal conductivity of fins, and decrease in fin spacing and wall heat flux.

Keywords: flow; heat transfer; staggered fins

Introduction

Flow separation caused by fins or sudden expansions creates reversed-flow regions of high mixing and turbulence levels. The boundaries of these reversed-flow regions are characterized by the creation and destruction of eddies of large turbulence energy. The separation of flow due to the presence of fins in channels is, therefore, of great interest to engineering applications and to the modellers of recirculating flows. The flow over fins is similar to the geometry of shell-and-tube heat exchangers and of corrugated channels. The features of such a flow involve curved shear layers, separation, and reattachment, plus stagnation, recirculating, and boundary-layer regions.

Fins provide an additional surface area for heat transfer. The fins cause the flow to deflect and impinge on the opposite wall and its fins, resulting in higher heat transfer coefficients than those obtained in the corresponding smooth duct. In general, the staggered fins cause more cross-flow than any other type of fins, and they are frequently found in commercial heat exchangers. The amount of cross-flow and extent of stagnant regions depends on the fin spacing and the size of fin overlap.

Previous numerical studies by Amano (1985) and Amano et al. (1987) provide flow and heat transfer characteristics in a periodically corrugated wall channel for both laminar and turbulent flows, respectively. Heat transfer characteristics of laminar constant-property fluid flow were analyzed in a parallel-plate channel with staggered, transverse ribs and a constant heat flux along both walls by Bennet and Myers (1983), Webb and Ramadhyani (1985), and Kelkar and Patankar (1987). Computations of turbulent flows were carried out in the periodic-flow regions for different Reynolds numbers, Prandtl numbers, and geometric arrangements by Habib et al. (1988). Experimental work was performed to determine local Nusselt numbers in the region beyond an abrupt expansion of a circular channel by Zemanick and Dougall (1970), Boyle (1984), Ichimiya (1987), Gunter et al. (1947), Knudsen and Katz (1985), Gay and Williams (1968), and Gay et al. (1977). These studies described experimentally the characteristics of the local heat transfer and the flow in the developing region by using air as a fluid when roughness elements are placed on the insulated wall.

The experimental measurements of complex turbulent flow fields in a model of the shell side of an axisymmetric heat exchanger with disk–doughnut baffles located in a water turbulent pipe flow by Founti and Whitelaw (1981) and in a two-dimensional (2-D) duct with segmental baffles by Berner et al. (1984) and Habib et al. (1984) indicate the significant influence of the baffle spacing on the flow features. A recent study by Mobarak et al. (1991) of the flow and heat transfer across segmental baffles indicates significant effect of baffle height and baffle material inside a rectangular duct on the flow pattern, heat transfer, and pressure drop for a fixed baffle spacing. Augmentation of heat transfer was obtained with increase in the Reynolds number, thermal conductivity of baffle, and baffle height.

In the present work, the turbulent flow and heat transfer in a rectangular duct with staggered fins are studied experimentally to investigate the effect of fin spacing and material on the heat transfer, the flow pattern, and pressure loss coefficients. The fin spacing ratios of 0.8, 1.5, and 2 are used with constant fin-height ratio of 0.7. The investigated Reynolds numbers ranged from 8,000 to 18,000.

Test rig and measuring instruments

The test rig and test section are shown in Figures 1 and 2, respectively. The test section is of rectangular cross section of 300 × 60 mm and is 1.0 m long; it consists mainly of a main duct, heaters, insulating materials, and electric power supply.

Address reprint requests to Professor Habib at the Mechanical Engineering Department, King Fahd University of Petroleum and Minerals, Box No. 1570, Dhahran 31261, Saudi Arabia.

Received 27 November 1991; accepted 27 July 1992

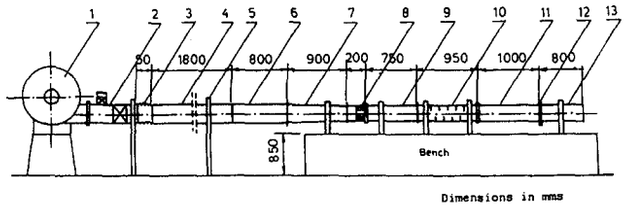

Figure 1 The test rig. 1: Air blower; 2: bypass section; 3: rubber joint; 4: PVC circular tube; 5: wooden support; 6: diffuser; 7: converging section; 8: honeycomb; 9: straight duct; 10: test section; 11: first segment of orifice meter; 12: orifice plate; 13: second segment of orifice meter

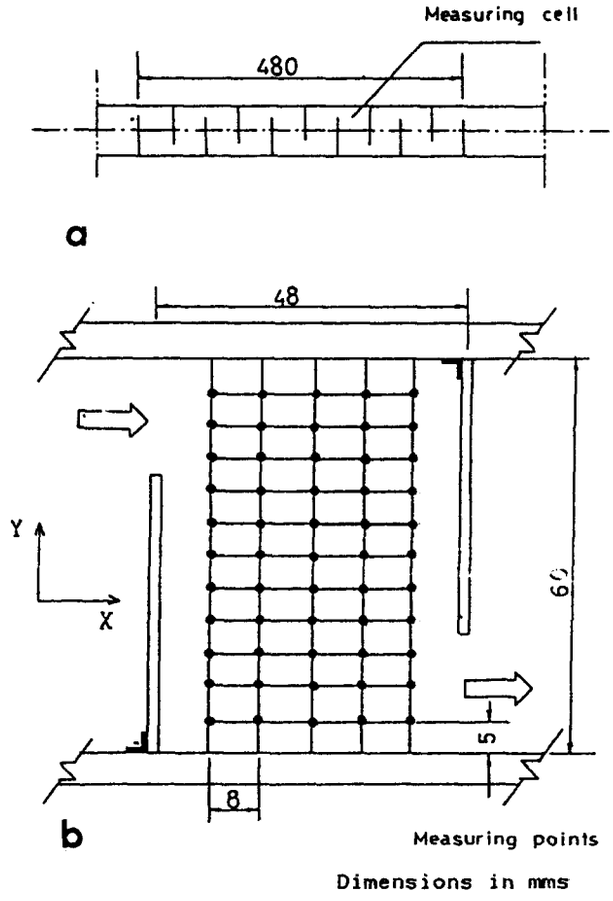

Figure 2 (a) The test section; (b) details of the cell and measuring locations

The test section is made from aluminium. The top and bottom plates are 6 mm thick and 330 mm wide, and the two sides are 1.5 mm thick and 60 mm deep. Both top and bottom surface plates are heated by electric heaters, while the two sides are adiabatic. The heater is controlled by a variac transformer, which provided a controllable constant heat flux for the test plate surfaces.

The fins are located alternatively at the top and bottom plates through grooves using silicon rubber to eliminate the air leakage. The main duct of the test section consists of consecutive cells. Four different test-section configurations are employed in the present work. They are tabulated in Table 1.

The pressure-drop measurements were obtained by a micromanometer to indicate the variation of pressure loss coefficient. Two pressure taps are located on the side of the test section upstream cell #6 and downstream cell #8. The pressure drop is indicated by a micromanometer Model MDC FG001. It has a range of 1,000 mm water with accuracy of ± 0.05 percent.

A five-hole probe with hemispherical head was used to measure the flow velocity. The air-flow velocity is measured at five sections across the test section on the horizontal section plane (see Figure 2). The velocity readings are taken at 11 sections with step 5 mm. Air-temperature measurements were taken and indicated by using Copper–Constantan thermocouples and data logger type Fluke Model 2200 B with ± 0.05°C accuracy. Surface temperatures were measured by 16 thermocouples inserted and soldered in holes in the surfaces.

Calculation procedure

The pressure loss coefficient was calculated from:

$$K = \Delta P/(1/2\rho U^2) \tag{1}$$

where u is the bulk flow velocity and ΔP is the pressure difference between two successive baffles on the same side. The entrance temperature T_{in} of air was measured using two thermocouples located at the inlet of the baffled test section. The bulk temperature T_b of air was calculated from the equation

$$T_b = \int_0^D |u| T dy / \int_0^D |u| dy \tag{2}$$

where u and T are the local velocity and temperature, respectively. The bulk temperature is calculated inside a periodic-flow cell (cell #7) for five sections in the axial direction of the flow. The wall heat flux, q, is calculated as follows:

$$q = Q/2WL \tag{3}$$

where Q is the wall heat flow and $2WL$ represents the surface area of the top or bottom walls. The local heat transfer

Notation

C	Total mean velocity
D	Channel height
H	Fin height/channel height
h	Heat transfer coefficient
K	Pressure-loss coefficients
Nu	Nusselt number
$\overline{\text{Nu}}$	Average Nusselt number
Nu_0	Nusselt number for fully developed laminar pipe flow
P	Pressure
q	Wall heat flux
Re	Reynolds number
S	Fin spacing
t	Fin thickness
U	Mean horizontal velocity
W	Channel width
X	Horizontal distance
Y	Vertical distance
ρ	Density

Table 1 Test-section configurations

Geom.	Exp No.	S/D	C/D	t/D	Baffle material	Volume-flow rate (lit/s)	Re No.	Heat flux (W/m^2)
(1)	1	0.8	0.3	0.025	Aluminum	27.3	8,140	3,971
	2					37.2	11,120	
	3					46.2	13,940	
(2)	4	1.5	0.3	0.025	Aluminum	27.3	8,140	3,971
	5					37.2	11,120	
	6					46.7	13,940	
	7					52.0	15,500	
(3)	8	2.0	0.3	0.025	Aluminum	27.3	8,140	3,971
	9					37.2	11,120	3,971
	10					46.7	13,940	3,971
	11					53.0	15,820	3,971
	12					57.5	17,380	3,971
	13					37.2	11,120	2,132
	14					37.2	11,120	991
(4)	15	2.0	0.3	0.025	Wood	27.3	8,140	3,971
	16					37.2	11,120	
	17					46.7	13,940	
	18					53.0	15,820	

coefficient, h, is then evaluated from the following equation:

$$h = q/(T_w - T_b) \tag{4}$$

where T_w is the wall temperature. The Nusselt number Nu was calculated, based on the hydraulic diameter D_h at the center of the cell, as follows:

$$\mathrm{Nu} = hD_h/k \tag{5}$$

The average Nusselt number for a single wall in the typical cell is given by

$$\overline{\mathrm{Nu}} = \bar{h}D_h/k \tag{6}$$

where

$$\bar{h} = 1/S\int_0^S h\,dx$$

To obtain the average Nusselt number for the cell flow, the heat transfer for both walls was taken into account.

The uncertainty estimation method by Kline and McClintock (1953) was used and indicates that the maximum uncertainties in the pressure loss coefficient and Nusselt number are 8.0 percent.

Results

The heat transfer coefficients are presented in terms of the ratio of the finned duct to the unfinned duct, $\mathrm{Nu}/\mathrm{Nu}_o$, where Nu_o is the fully developed laminar-flow Nusselt number (Holman 1981). The results are arranged in four groups according to the geometry of the tested cell. These geometries correspond to the 18 experiments indicated in the experimental program of Table 1. The results present the influence of the Reynolds number, geometry, fin material, and heat flux on the heat transfer coefficients.

Influence of Reynolds number

Figure 3 presents the velocity contours for different Reynolds numbers. The field is a turbulent shear flow, which is characterized by a large recirculation zone upstream of the left fin with flow upward near the left fin and downward near the right baffle. The size of the reversed flow region increases slightly with the Reynolds number, causing the through flow

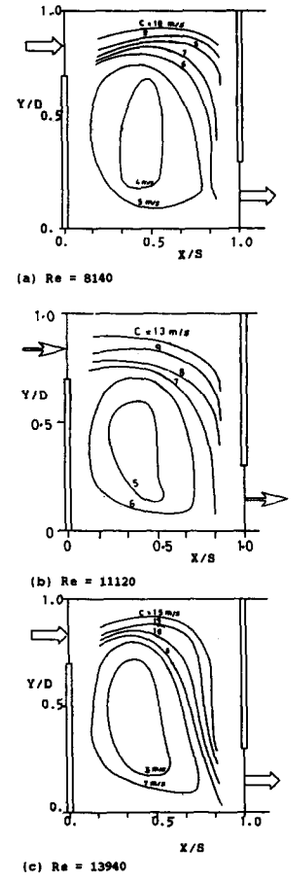

Figure 3 Influence of Reynolds number on the flow pattern at $S/D = 0.8$

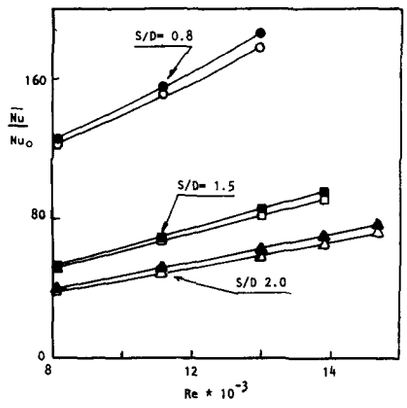

Figure 4 Effect of Reynolds number on the average Nusselt number. Closed symbols: top wall; open symbols: bottom wall

to bend more significantly, as confirmed by Kelkar and Patankar (1987) and Habib et al. (1988).

The influence of the Reynolds number on the average heat transfer coefficient is shown in Figure 4 for different geometries. The figure indicates that the top wall has higher values of the average Nusselt number than the bottom wall for all S/D values. This may be attributed to the high velocity values at the top wall as given by Figure 1. Consequently, the heat transfer coefficients are high.

General relations for average heat transfer coefficient for top and bottom walls in the periodic cell were obtained for aluminium fins at $H/D = 0.7$:

$$\overline{Nu} = 0.2683(S/D)^{-1.2}\ Re^{0.8}$$

and for wood fins at $S/D = 2.0$, $H/D = 0.7$:

$$\overline{Nu} = 0.115\ Re^{0.8}$$

Influence of fin spacing

Flow field. The effect of fin spacing on the flow field is shown in Figure 5. The effect of reducing the fin spacing is qualitatively very similar to increasing the Reynolds number. As fin spacing decreases, the relative strength and size of the recirculation zone grow, causing the through flow to bend more significantly.

Periodicity. Figure 6 shows the effect of fin spacing on the periodicity for $Re = 8140$. The figure indicates that, for $S/D = 0.8$, the flow must pass through three cells before it becomes a thermally periodic, fully developed flow. For $S/D = 1.5$, five cells are needed, while six cells are needed for $S/D = 2.0$ for the flow to achieve the thermally periodic fully developed state.

Local Nusselt number. The effect of fin spacing on the local Nusselt number over the top and bottom walls of the periodic cell is shown in Figure 7. The Nusselt number for both top and bottom walls is generally reduced with fin spacing. The effect of increasing the fin spacing is qualitatively very similar to decreasing Reynolds number. The impingement and strength of the reversed flow decreases with fin spacing and thus leads to reduced Nusselt numbers. For the top wall, the increase in the fin spacing ratio S/D from 0.8 to 2.0 leads to a reduction in the Nusselt number over the whole top surface, as shown in Figure 7.

Average Nusselt number. Figure 8 shows the variation of average Nusselt number for the top and bottom walls of the periodic-flow cell with fin spacing at different Reynolds

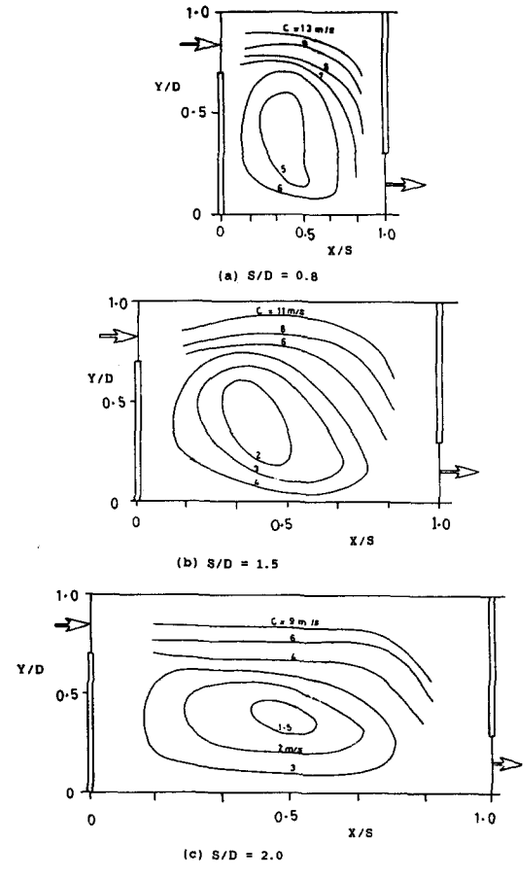

Figure 5 Influence of the fin spacing on the flow pattern at Re = 11,120

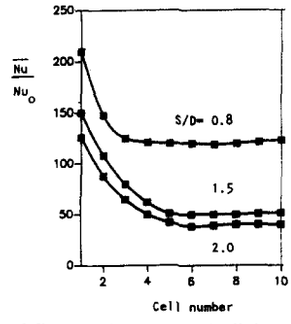

Figure 6 Effect of fin spacing on periodicity at Re = 8,140 with aluminium fins

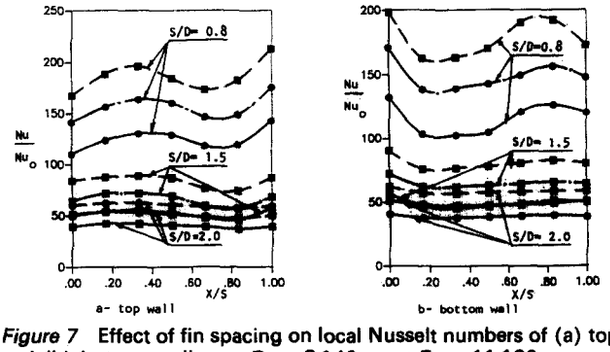

Figure 7 Effect of fin spacing on local Nusselt numbers of (a) top and (b) bottom walls. —: Re = 8,140; –·–: Re = 11,120; - - - - -: Re = 13,940

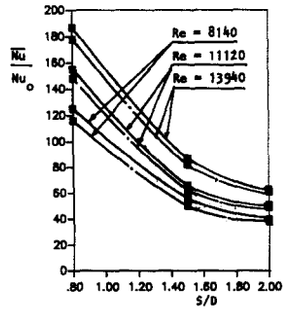

Figure 8 Effect of fin spacing on the average Nusselt numbers at different Reynolds numbers. —: top wall; –·–: bottom wall

numbers. A significant augmentation of heat transfer is achieved by insertion of fins. Augmentation of heat transfer was obtained with Reynolds number and with decreasing the fin spacing. As the fin spacing becomes larger, the behavior approaches that of an unfinned duct.

Overall average Nusselt number and pressure loss coefficient. Figure 9 shows the effect of the fin spacing S/D on overall average Nusselt number and pressure loss coefficient for the periodic cell at different Reynolds numbers. A maximum overall average Nusselt number occurs at a fin spacing of $S/D = 0.8$. As the fin spacing decreases, the pressure loss coefficient increases. The results show that, for fin spacing S/D between 0.9 and 1.2, the pressure loss coefficient is relatively low while the Nusselt number is relatively high. For fin spacing larger than $S/D = 1.5$, the average Nusselt number becomes very low due to the weakness of impingement flow and recirculating zones. For baffle spacing less than $S/D = 1.0$, the increase in the pressure loss coefficient is higher than the increase in heat transfer.

The results indicate that the average Nusselt number increases with decreasing the fin spacing. Figure 9 also shows that the heat transfer is augmented by about 31.0 percent, and the pressure drop coefficient is increased by 12.0 percent only as a result of decreasing of fin spacing from $S/D = 2.0$ to $S/D = 1.5$ at Re = 11,120. Further decrease of S/D to 1.0 causes an increase in heat transfer coefficients and reduction in pressure drop by 75 percent and 38 percent, respectively. These figures are 33 percent and 48 percent, respectively, as S/D is reduced from 1.0 to 0.8.

The reason for the large pressure drop is due to the significant distortion of the flow caused by the fins, especially

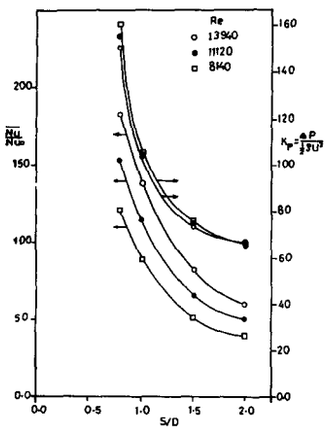

Figure 9 Variation of average Nusselt number and pressure-loss coefficient with fin spacing

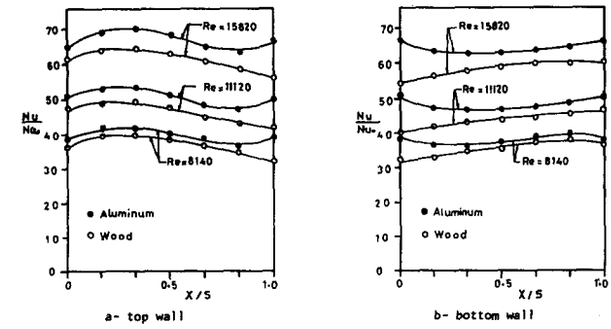

Figure 10 Effect of fin material on the local Nusselt number at $S/D = 2.0$

for the narrow fin space. This same distortion produces flow impingement on the front face of the fins and on the tested cell walls, leading to the increased heat transfer.

Influence of thermal conductivity of fin

The effect of thermal conductivity of the fins on the variation of the local Nusselt number for the top and bottom walls is shown in Figure 10 for different Reynolds numbers. The thermal conductivity of the fins has a significant influence, especially near the base of the fin, near $X/S = 1.0$ for the top wall and $X/S = 0.0$ for the bottom wall. In this region, the local heat transfer is largely influenced by the thermal conductivity.

In general, the heat transfer increases with the thermal conductivity of the fins. This is because, in case of high thermal conductivity, heat is allowed to transfer through the fins. In the case of wood fins, the heat is prevented from passing through the wood fins, as confirmed by Habib et al. (1988).

Influence of the heat flux

Local heat transfer coefficient. The effect of heat flux on local Nusselt number for the top and bottom walls of the tested cell is shown in Figure 11 for aluminium fins at Reynolds number of 11,120, $S/D = 2.0$, and $H/D = 0.7$. The heat flux is reduced to 65 percent and then to 32.5 percent of its original value. The local Nusselt number increases as the heat flux decreases. This is due to the reduced surface temperature as the heat flux decreases. Consequently, the thickness of the thermal boundary layer decreases and the difference between flow and wall temperature is reduced, thus resulting in an increase of the heat transfer coefficient.

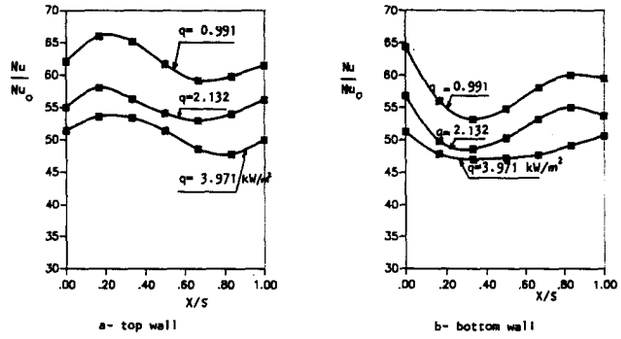

Figure 11 Effect of heat flux on the local Nusselt number at Re = 11,120

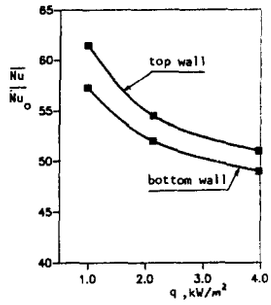

Figure 12 Effect of heat flux on the average Nusselt number at $S/D = 2.0$

Average heat transfer coefficients. The effect of heat flux on the average Nusselt number for both top and bottom walls is shown in Figure 12. The average Nusselt number increases as the heat flux decreases. The figure shows that, by decreasing the heat flux to 65.0 percent (see previous paragraph), Nu increases by 8.2 percent, and by decreasing the heat flux to 32.5 percent, Nu increases by 20.8 percent. The difference in Nusselt number between the top and bottom walls is due to the impingement of the flow on the top wall of the tested cell. It is also due to the fact that the bottom wall is covered by the main recirculation zone as indicated before.

Conclusions

The main conclusions are as follows:

(1) the development length necessary to achieve a streamwise-periodic flow is a function of the Reynolds number and fin spacing;
(2) the relative strength and size of the recirculation zone grow as Re increases, causing the through flow to bend more significantly;
(3) reducing the fin spacing is qualitatively very similar to increasing Re;
(4) the heat transfer coefficient increases with decreasing the heat flux and increasing the thermal conductivity of the fins;
(5) empirical relations for heat transfer coefficients for the tested cell were obtained for aluminium and wood fins;
(6) pressure-loss coefficients increase with increasing Reynolds number and decreasing fin spacing; and
(7) the local and average heat transfer coefficient increase with Re and thermal conductivity of the fins, and with decreasing the heat flux.

Acknowledgment

The authors would like to acknowledge the support by Cairo University and King Fahd University of Petroleum and Minerals for this research project.

References

Amano, R. S. 1985. A numerical study of laminar and turbulent heat transfer in periodically corrugated wall channel. *J. Heat Transfer*, **107**, 564–569

Amano, R. S., Bagherlle, A., Smith, R. J., and Niess, T. G. 1987. Turbulent heat transfer in corrugated wall channels with and without fins. *ASME J. Heat Transfer*, **109**, 62–67

Bennet, C. O. and Myers, J. E. 1983. *Momentum, Heat, and Mass Transfer*. McGraw-Hill, New York

Berner, C., Durst, F., and McEligot, D. M. 1984. Flow around baffles. *J. Heat Transfer*, **106**, 743–749

Boyle, R. J. 1984. Heat transfer in serpentine passages with turbulence promoters. ASME Paper No. 84-HT-24

Founti, M. A. and Whitelaw, J. H. 1981. Shell-side flow in a model disc-and-doughnut heat exchanger. Imperial College Technical Report Fs/81/37, London

Gay, B., Jenkins, J. D., and Mackley, N. V. 1977. Shell side heat transfer coefficients in cylindrical heat exchangers; the influence of geometrical factors. I. The non-leakage case. *Lett. Heat Mass Transfer*, **4**, 41–52

Gay, B. and Williams, T. A. 1968. Heat transfer on the shell-side of cylinder shell-and-tube heat exchanger fitted with segmental baffles. *Trans. Inst. Chem. Eng.*, **46**, T95–T100

Gunter, A. Y., Sennstrom, H. R., and Kopp, S. A. 1947. Study of flow patterns in baffled heat exchanger. ASME paper 47-A-103

Habib, M. A., Attya, A. M. and McEligot, D. M. 1988. Calculation of turbulent flow and heat transfer in channels with streamwise-periodic flow. *ASME J. Turbomachinery*, **110**, 405–411

Habib, M. A., Durst, F., McEligot, D. M. 1984. Streamwise-periodic flow around baffles. *Proc. 2nd Int. Conf. Appl. Laser Anemometry to Fluid Mech.*, Lisbon, Portugal

Holman, J. P. 1981. *Heat Transfer*. McGraw-Hill, New York

Ichimiya, K. 1987. Effects of several roughness elements on an insulated wall for heat transfer from the opposite smooth heated surface in parallel plate duct. *ASME J. Heat Transfer*, **109**, 68–73

Kelkar, K. M. and Patankar, S. V. 1987. Numerical predictions of flow and heat transfer in a parallel plate channel with staggered fins. *ASME J. Heat Transfer*, **109**, 25–30

Kline, S. J. and McClintock, F. A. 1953. Describing uncertainties in single sample experiment. *Mech. Eng.*, **75**, 3–8

Knudsen, W. W. and Katz, D. L. 1985. *Fluid Dynamic and Heat Transfer*. McGraw-Hill, New York

Mobarak, A. M., Habib, M. A., Abdel-Hafez, E., El-Salak, M., and Afify, R. I. 1991. Turbulent flow and heat transfer in rectangular duct with segmental baffles of different heights. *J. Helwan Univ.* **1**, 1, Egypt, 1–12

Webb, B. W. and Ramadhyani, S. 1985. Conjugate heat transfer in channel with staggered ribs. *Int. J. Heat Mass Transfer*, **28**, 1679–1689

Zemanick, P. P. and Dougall, R. S. 1970. Local heat transfer downstream of abrupt circular channel expansion. *ASME J. Heat Transfer*, **92**, 53–60